Magneto-optical Kerr studies on thin films and Nanoparticles.

A thesis submitted in partial fulfillment of the requirements for the degree of Bachelor of Science in Physics from the College of William and Mary in Virginia,

By

Andrew Nelson

Research Advisor, Professor Ale Lukaszew

Williamsburg, VA

December 2009

Abstract

The focus of this research was to characterize the behavior of two different ferromagnetic structures, thin films and nanoparticles, through the magneto-optical effects. The magneto-optical Kerr Effect (MOKE) was used to characterize the crystalline structures of Nickel (Ni) thin films epitaxially grown on a Magnesium Oxide substrate Crystalline, Ni films were of interest for subsequent ultra-fast time-resolved studies within professor Luepke's group. The Faraday Effect was used to measure the magneto-optical properties of nanoparticles which have a Fe-Ag core-shell microstructure to explore novel sensing platforms. Several samples which differed in ratio of Fe to Ag composition were used to characterize how the particles behave. It is expected that the noble metal (Ag) may induced enhancement of the magneto-optical activity. This is due to localized surface plasmons, i.e. charge oscillation in the conductor that give rise to large EM fields in the core of the sample. This in turn exposes the magnetic materials to larger fields leading to enhanced magneto-optical response. These studies may lead to optimized sensing applications.

Table of Contents

Chapter **Page**

I. Acknowledgements

I would like to thank all the people who have made my academic career possible. I would especially like to thank Professor Ale Lukaszew for her unwavering and continued support. Thank you for pushing me and for opening so many doors for me. You have opened my eyes to paths and options in my life that I didn't know existed. I cannot express my gratitude for everything you have done for me.

To my parents, I want to thank you for not only giving me the opportunities you have, but for how you have never once expressed doubt in my abilities to do whatever I wanted with my life. I also want to thank you for constantly pushing me to do my best. I love you both very much.

To Jonathan Skuza, I would like to thank you for taking time to show me everything. Thank you for teaching me how to set up and run the apparatus last year. I sincerely hope I was not too much of a bother for you.

To the rest of Professor Lukaszew's team I would like to thank you for all of your support. Whether we worked together or you listened to presentations I gave at our group meetings, being there helped me in more ways than you may know.

I would like to give my thanks to the late Professor Michael Finn. While he did not help me on this project he was a great inspiration to me in many other ways. No one has inspired me the way that you did. Thank you very much.

I apologize to anyone I did not recognize here. Truth is almost everyone I have met has helped me in some way and deserves my gratitude and I deeply regret not being able to list them all by name.

II. Background and Theory

a) Ferromagnetism

Ferromagnetism is a physical trait exhibited by certain materials. Ferromagnetic materials keep an internal magnetization, average "spin" orientation, even in the absence of a magnetic field.[3] An atom's magnetic moment is caused by its electron's spin and orbital angular momentum. When the magnetic moments of many unpaired electrons are aligned in the same direction a macroscopic magnetic field can be observed. It is implied then that not all materials can exhibit ferromagnetism, only those with unpaired electrons in the valence shells. Interestingly ferromagnetism shows anisotropic properties when certain materials have a specific shape or crystallographic form. Several elements in the periodic table including Fe, nickel (Ni), and cobalt (Co) exhibit ferromagnetism.[2] There are other materials that are ferromagnetic including a few rare earth elements.

Spin is a quantum mechanical property. Ferromagnetism occurs when the unpaired electrons from neighboring electrons from two or more atoms are coupled through the exchange interaction. When this happens the electrons align their magnetic moments parallel to eachother. This accounts for the internal magnetic field observed in ferromagnets even in the absence of externally applied fields.[2] It is not until the material is subjected to a strong enough external magnetic field and thereby magnetized that these moments align uniformly throughout the material.

To magnetize a sample material, it must be subjected to a strong external field. In doing this the electrons spin and magnetic dipoles align parallel to and in the same direction as the external field. [3] The reversal of the magnetization direction can be achieved by reversing the direction of

the applied field. Figure 1 shows a material with three different magnetizations (Note: the intermediate demagnetized state may also exhibit domain structure, not indicated here). The arrows are a representation of the direction of the dipole of the substances. The arrows do not represent magnitude of the dipoles only direction.

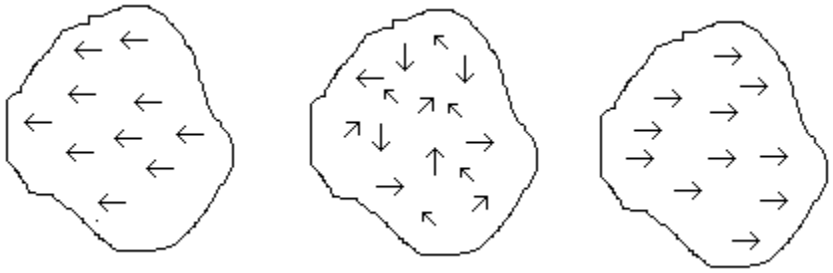

Figure 1

Ferromagnets can have a magnetic anisotropy which is dependent upon many factors. The anisotropy will determine along which axis the material can be magnetized easily. Along the hard axis, the material will require a larger magnetic field to align all the spins. The anisotropy can be dependent upon the bulk material's shape, and if the material is a crystal then its crystalline structure. This anisotropy can be measured through hysteresis for example.[2]

b) Ferromagnetic Hysteresis

A hysteresis loop is a graph of the magnetization process followed by the reversal process. In most magnetic materials these two processes are path-dependent and therefore hysteretic. Figure 2 is an example of multiple hysteresis loops of an internal magnetization versus the strength of an external magnetic field. [4]

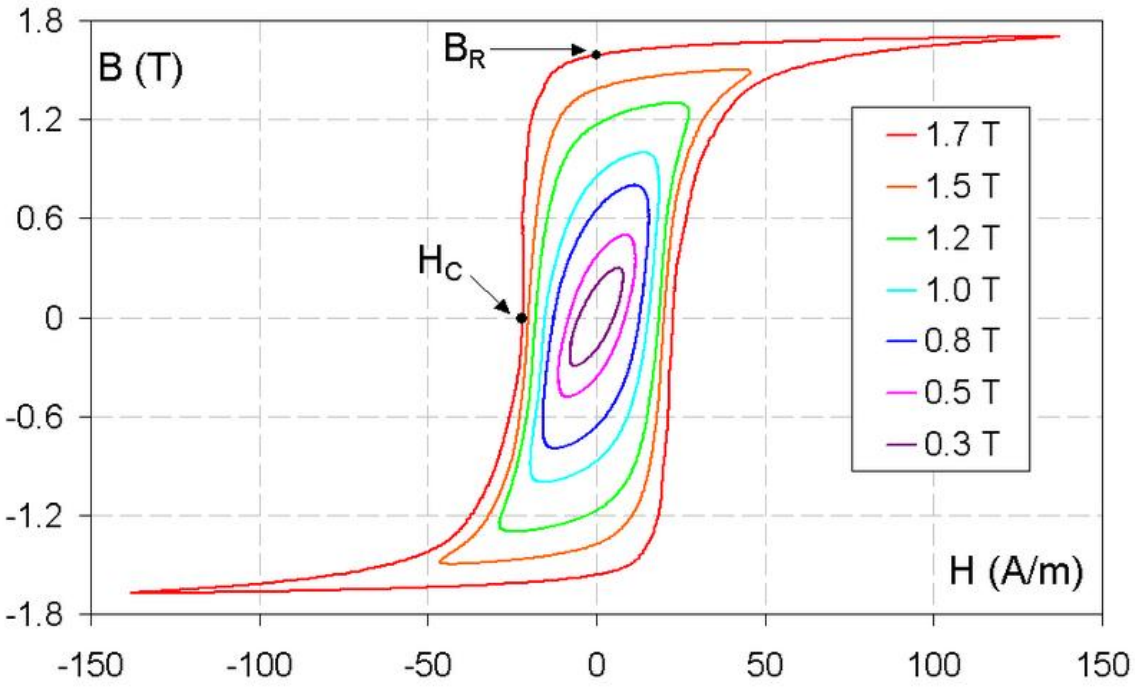

Figure 2

Figure 2 shows minor loops, ones where the sample does not reach saturation before reversal, and the full hysteresis loop upon saturation, which is the largest loop. There are two points of interest on this latter graph. The B_R is the remanence field. This is the internal magnetization of the material when the applied external magnetic field is reduced to zero from the saturation value, or the 'field that remains'. Notice that there are two values for the B_R though both are about the same intensity they are in opposite directions. The first value is obtained after saturating the magnetization in a given orientation and then reducing the applied field to zero. Upon increasing the magnitude of the field in the opposite direction, the material is once more magnetized but in the opposite direction with respect to its previous state and the process is reversed to complete the hysteresis loop. Thus the magnetization can be changed if the substance is subjected to a strong enough field in the opposite direction. The second important value, the H_C, is the coercivity value. This is the necessary intensity of an external magnetic field to switch

the direction of the internal magnetization. Once again there are two values, one for each direction of the magnetic field. The coercivity, remanence, and the shape of the hysteresis loop are unique and material dependent and also depend on other specific characteristics such as the shape of the specimen, its crystallographic structure, etc. Thus, for the specific case of crystalline thin films, a study of the hysteresis loop properties for various in-plane crystallographic orientations reveals the character of the magneto-crystalline anisotropy and can be used as a test of the crystalline quality of a sample.[4]

c) Magneto-Optical effects

Maxwell's equations of electromagnetism as well as appropriate boundary conditions predict the behavior of light as it interacts with different surfaces. For the specific case of magnetic materials, the dielectric tensor exhibits non-zero off-diagonal elements that give rise to magneto-optical effects. The magnetization of ferromagnetic materials changes the permittivity tensor matrix in such a way that light will change its polarization when interacting with the surface of the material.[3]This gives rise to the magneto optical effects.

Light is an electromagnetic (EM) wave. This means that it has two components, an electric field and a magnetic field. The fields are perpendicular to each other and to the direction of motion of the wave, as in the figure 3.

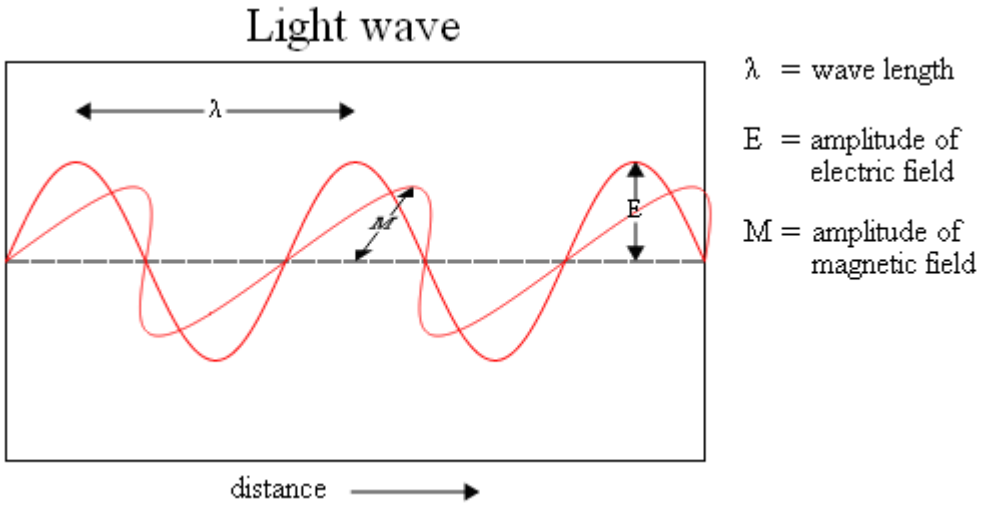

Figure 3

EM waves are said to be polarized when the electric field has a defined orientation. Light can be polarized in different ways, linearly, circularly, or elliptically as the following figure demonstrates.[3]

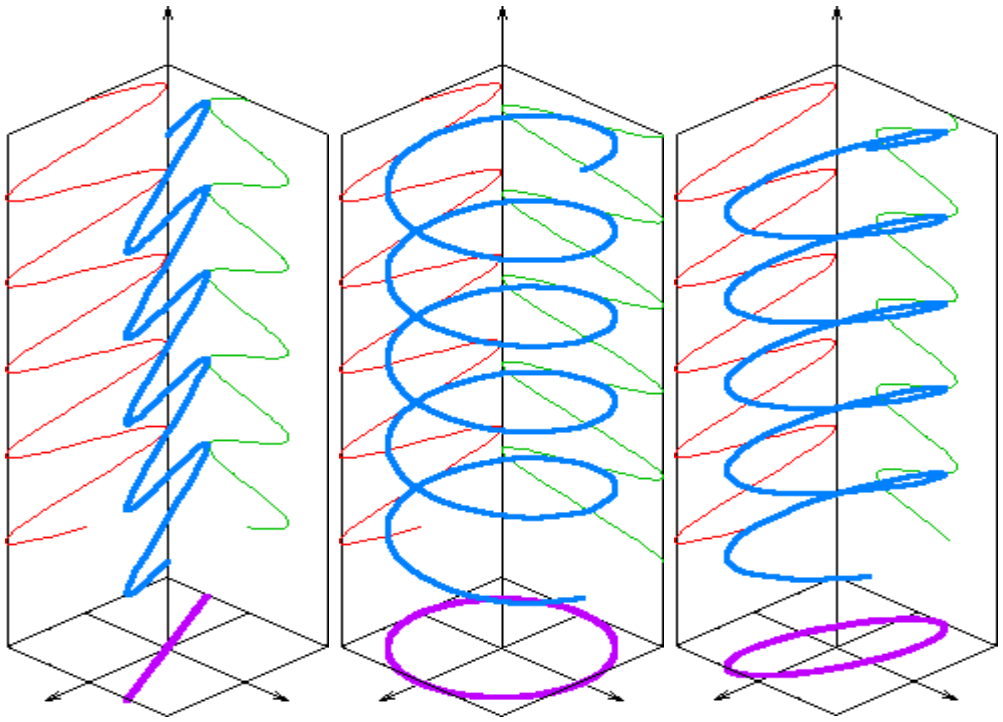

Figure 4

Figure 4 is a collection of Lissajous plots (purple) of the x-component (red) and the y-component (green) of the electric field (blue) of a polarized EM wave. In the case of linear polarization the x and y components are in phase and of equal amplitude. Circular polarization occurs when the two components are out of phase by ninety degrees but have equal amplitude. Elliptical polarization can occur when the two components are out of phase but not by ninety degrees, or the amplitudes of the two components are not equal.[10]

When polarized light interacts with a magnetic medium the polarization of the light can change. When the light interacts with an electron of the material the way the electron reacts adds additional components to the EM wave which alter its polarization. This interaction is the magneto-optical effect.[1]

Everything that has been presented so far up to the rotation of polarization can be explained with Maxwell's equations and appropriate boundary conditions. It follows then that the rotation in polarization can be predicted for a specific material with a given internal magnetization. The degree of rotation is called the Kerr angle.

Start with the pertinent Maxwell equations as in equation 1,

$$\nabla \times \mathbf{E} = -\frac{1}{c}\frac{\partial \mathbf{H}}{\partial t},$$

$$\nabla \times \mathbf{H} = \frac{1}{c}\frac{\partial \mathbf{E}}{dt} + \frac{4\pi}{c}\boldsymbol{\alpha}\cdot\frac{\partial \mathbf{E}}{\partial t} + \frac{4\pi}{c}\boldsymbol{\sigma}\cdot\mathbf{E}.$$

Equation 1

The EM wave propagating along the z axis will then be given by equation 2, where E_0 and H_0 are the maximum amplitude of the fields, ω is the angular frequency of the EM wave, *t* is time elapsed and c is the speed of light. *N* is an index of refraction, such that equation 3 holds true. In equation 3 k is a unit vector in the z direction and,

$$\mathbf{E} = \mathbf{E}_0 e^{i\omega(t - Nz/c)}$$
$$\mathbf{H} = \mathbf{H}_0 e^{i\omega(t - Nz/c)},$$

Equation 2

$$N(\mathbf{E} \times \mathbf{k}) = -\mathbf{H},$$
$$N(\mathbf{H} \times \mathbf{k}) = \mathfrak{A} \cdot \mathbf{E},$$

Equation 3

In equation 4, α_0 and σ_0 are tensors of conductivity and polarizability respectively.

$$\mathfrak{A} = \mathbf{1} + 4\pi\boldsymbol{\alpha} + \frac{4\pi}{i\omega}\boldsymbol{\sigma} = \begin{bmatrix} A_0 & -A_1 & 0 \\ A_1 & A_0 & 0 \\ 0 & 0 & A_0 \end{bmatrix},$$
$$A_0 = 1 + 4\pi\alpha_0 + \frac{4\pi}{i\omega}\sigma_0,$$
$$A_1 = 4\pi\alpha_1 + \frac{4\pi}{i\omega}\sigma_1,$$

Equation 4

Through substituting the value of H in equation 3the equation 5 is obtained.

$$\mathfrak{A} \cdot \mathbf{E} = N^2[\mathbf{E} - \mathbf{k}(\mathbf{E} \cdot \mathbf{k})],$$

Equation 5

Equation 5 has components of the form equation 6.

$$(A_0 - N^2)E_x - A_1 E_y = 0,$$
$$A_1 E_x + (A_0 - N^2)E_y = 0,$$
$$A_0 E_z = 0.$$

Equation 6

Taking the determinant of the components will give solutions for N^2 which are shown in equation 7.

$$N_+^2 = A_0 - iA_1,$$
$$N_-^2 = A_0 + iA_1.$$

Equation 7

The two solutions show that for N_+^2, $E_y^+ = +iE_x^+$ and for N_-^2, $E_y^- = -iE_x^-$. In other words a wave can travel either to the left or to the right along the z axis. After coming into contact with a magnetized media the wave will be reflected and refracted as well as elliptically polarized.

The reflected polarization angle is given by equation 8, and the refracted polarization angle is given by equation 9,

$$\phi_K = -\mathcal{I}[(N_+ - N_-)/(N_+N_- - 1)],$$

Equation 8

$$\phi_F = \tfrac{1}{2}(\omega z/c)\mathcal{R}(N_+ - N_-),$$

Equation 9

Then, substituting the following we have equation 10. [9]

$$N_+ - N_- = (-4\pi)\frac{(\sigma_1/\omega) + i\alpha_1}{n - ik},$$

$$\frac{N_+ - N_-}{N_+N_- - 1} = (-4\pi)\frac{(\sigma_1/\omega) + i\alpha_1}{(n - ik)[(n - ik)^2 - 1]}.$$

Equation 10

The magneto-optical effect is named differently depending on whether the light is being reflected or transmitted through the sample. If the light is being reflected the effect is called the magneto-optical Kerr Effect. If the light is transmitted it is referred to as the Faraday Effect.[1]

The magneto-optical Kerr effect can be measured in one of three different geometries; longitudinal, polar, or transverse. Figure 5 illustrates these three orientations for MOKE.

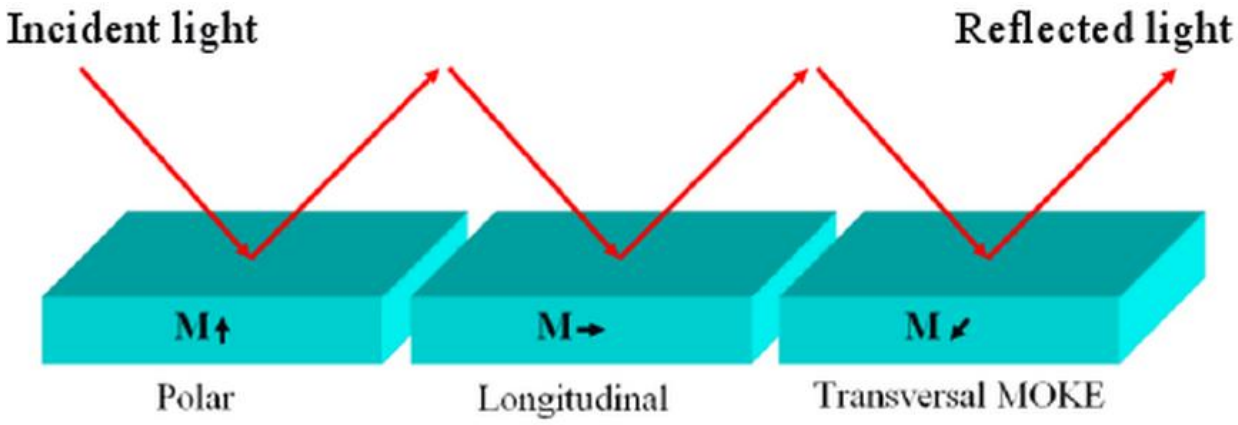

Figure 5

The polar configuration is used when the magnetization is perpendicular to the sample plane. In the longitudinal and transverse orientations the magnetization is in the plane of the sample and parallel or perpendicular to the plane of incidence respectively. [6]

d) Thin Films

In a thin film, one of the three dimensions is only a few nanometers thick. If the thin film is a ferromagnet, its magnetization is generally in the plane of the sample due to the 'shape' anisotropy. The shape anisotropy favors configuration which minimize the magnetic charge on a surface. This allows the sample to be studied using transverse or longitudinal MOKE in the particular case of Ni thin films. If the film is crystalline, rich information regarding the in-plane magneto-crystalline anisotropy can be obtained through magneto-optical studies.

e) Nanoparticles

A nanoparticle is defined as any particle that has all three dimensions between 1 and 100 nanometers.[7] Fe nanoparticles have been shown to have their magneto-optical characteristics

increased when coated with a noble metal.[5] This is due to the fact that the optical properties of gold and silver are such that these materials can sustain strong Surface Plasmon resonances at visible wavelengths leading to strong electromagnetic fields in the core of the nanoparticles. Thus when a noble metal, such as Ag, is coated around a Fe core a dramatic increase in the magneto-optical effect is expected. It is then of interest to find how the effect is enhanced by changing the ratio of Fe to Ag for possible sensing applications.[5]

III. Experimental

a. Magneto-Optical Kerr Effect on thin films

The aim was to measure the magnetocrystalline anisotropy of a nickel thin film grown on a magnesium-oxide substrate. MOKE in the longitudinal geometry was used because the magnetization of the sample was in the sample's plane. Transverse was not used due to the increased complexity of the orientation. Figure 6 is picture of the experimental setup.

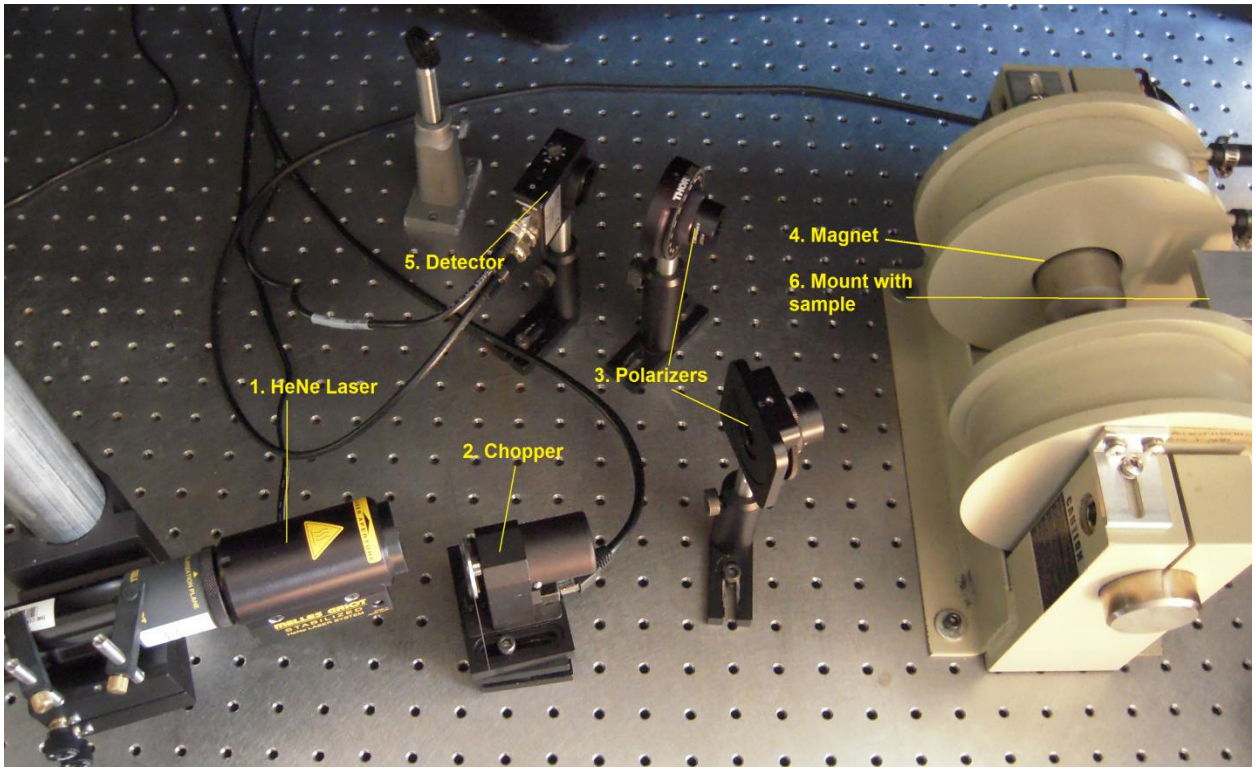

Figure 6

This is the actual set up used in the laboratory. The setup was optimized to increase signal to noise ratio in the measured signal. The detector and the chopper were both connected to a lock-in amplifier to ensure that only light reflected from the sample was being measured. This was done through lock-in technique. The chopper would parse the signal at a particular frequency which would allow the lock-in amplifier to pick out the reflected light from the background light.

The light source was a HeNe laser. The first polarizer the light encountered was used to ensure that the light was linearly polarized. The second polarizer was crossed with the first in order to apply the "null method", by which small changes in light- intensity can be measured against a low background as opposed to a large background that would be close to the detector saturation. A lab view interfaced computer was connected to the lock-in amplifier, the electromagnet, and the stepping motor sample holder allowing in-plane rotation of the sample.

The sample was mounted by carefully placing double-sided tape to the back of the sample. The sample was then handled with tweezers and lifted from the side to prevent damage to the surface. It was then placed on the axis of the sample-holder rod, which was connected to a stepping motor allowing controlled axial rotation. The tweezers were then used to gently press on the outer edges of the sample to make sure the sample was parallel to the surface of the rod's end. The setup was aligned such that as the sample rotated, the reflected light would always be on the photo-diode and the plane of the sample parallel to the external applied field.

The setup was used to measure a hysteresis loop for the sample at a specific in-plane orientation of the magnetic field; the sample was then rotated by a predetermined angle, and another hysteresis loop measured and so on. After a full 360 degree rotation the coercive values from the individual hysteresis loops could be plotted in an azimuthal map. The azimuthal map could then be used to assess the crystalline quality of the nickel thin film sample grown on (001) oriented magnesium oxide.

b. Magneto-optical Faraday Effect on nanoparticles

The following is a figure of the experimental setup.

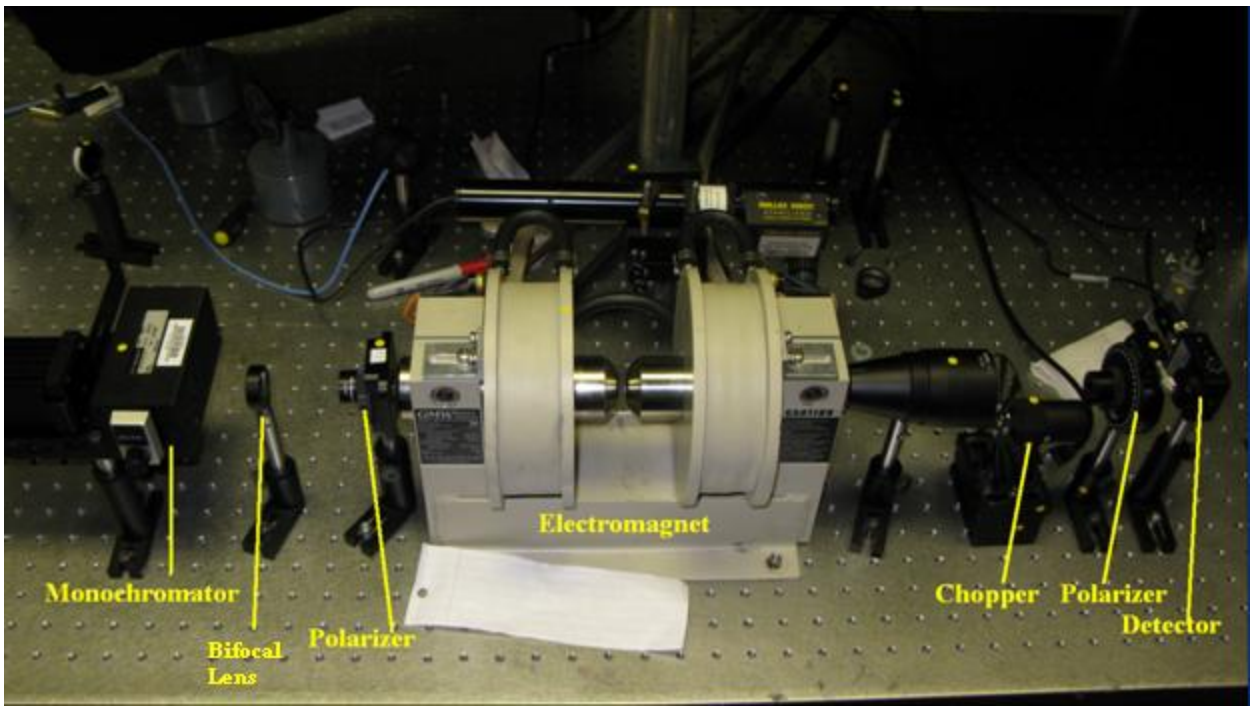

The main differences with respect to the previous setup is that the second polarizer, the chopper, and the detector were all placed at the opposite side of the material, and instead of a laser, a polychromatic light source with a monochromator was used to measure the Faraday rotation angle versus wavelength. In addition, a bored polar piece was used in the electromagnet to allow for the required transmission geometry while still providing sufficient magnetic field on the sample. The same Lock-In technique was used for the measurements, with the light modulated with a chopper. For this geometry, the two polarizers were not crossed but formed an angle of 45 degrees from each other. The incident and transmitted light was substantially weaker than the light from the HeNe laser so the null effect was not used. Because of the geometry of the

sample (nanoparticles dispersed in a liquid) the angular dependence of the magneto-optical properties was not measured.

The sample was mounted on a glass slide. Fe-Ag core-shell nanoparticles with a 25:75 ratio were placed on the glass. Oil of the same refraction index as the glass substrate, n=1.5018, was then used to prepare a suspension, and to uniformly spread it on the slide. A glass cover was then placed on top of the sample and the oil-nanoparticle mixture. This was placed in a clamp and the clamp was placed between the two electromagnetic poles. It was then oriented to maximize the signal detected by the photodiode.

Once the sample was mounted the measurements began. The operator would set the wavelength to a predetermined value and take two readings, one with the magnet on and one with the magnet off. Prior hysteresis loops obtained with VSM magnetometry indicated that the strength of the external magnetic field needed to be 1 Tesla to ensure the nanoparticles were saturated and therefore produce the maximum magneto-optical effect. After both readings were taken the wavelength would be systematically changed a predetermined amount and the process was repeated to obtain all the pertinent data for a spectrum of Faraday rotation versus wavelength.

IV. Results and Conclusions

a. Magneto-Optical Kerr Effect on thin films

The azimuthal plot obtained from the experiment is shown below.

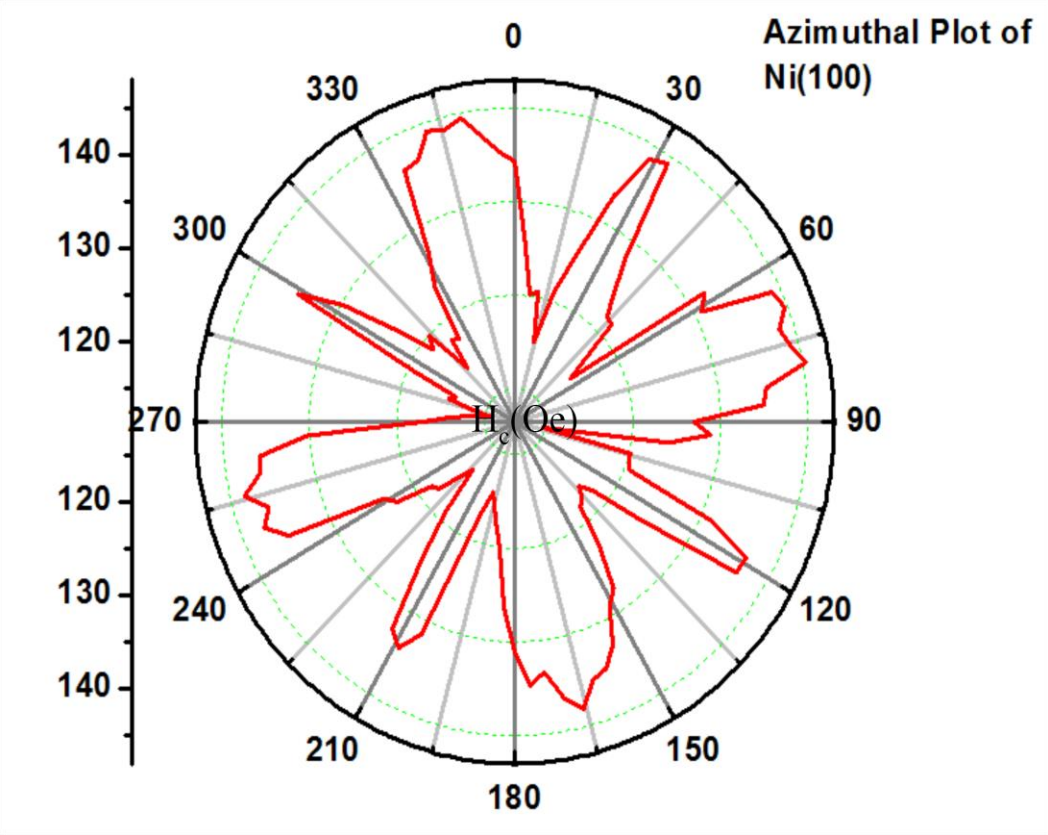

The four fold symmetry is expected for a (001) oriented face cubed centered nickel crystal. The sample exhibited good crystalline quality and was then sent to Kevin Smith in Professor Luepke's group to be used in time-resolved MOKE studies towards his doctoral thesis.

b. Magneto-optical Faraday Effect on nanoparticles

The core-shell Ag-Fe nanoparticles sample exhibited a large enhancement of magneto-optical effects as compared to the expected effect for pure Fe nanoparticles samples. The following graphs show that there is a maximum of absorption and Faraday rotation around the 3eV band. Thus, there is a strong correlation between the strong absorption due to localized surface plasmons and the magneto-optical activity.

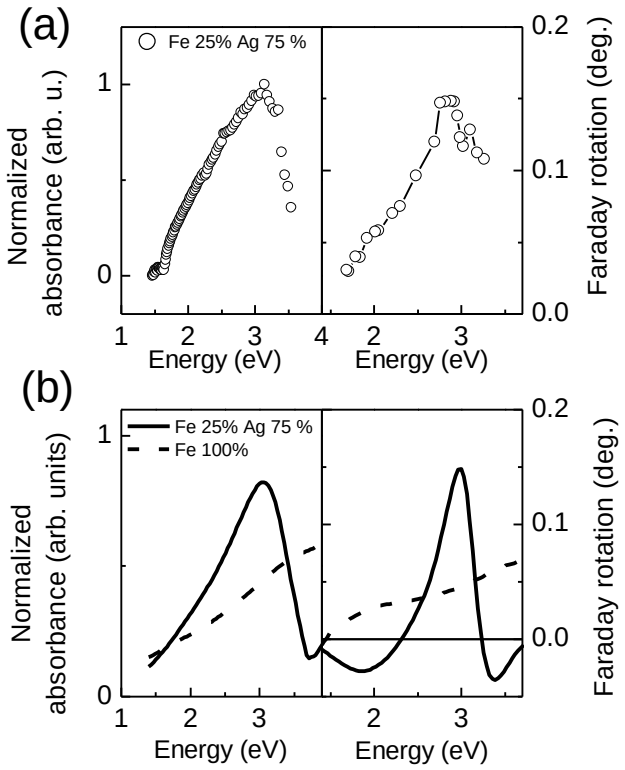

The top two graphs show the actual data from the experiment. The right graph is the absorption and the left graph is the Faraday rotation of the wave. The bottom two graphs are simulations

that were done to predict the behavior of the sample and to compare with the expected rotation for pure Fe nanoparticles. The solid line represents the sample with the 25:75 ratio while the dotted line represents a sample composed of pure Fe. Experiments with pure Fe nanoparticles were not possible because of the strong tendency of this material to oxidize. Our results are consistent with similar findings on Au-Ferrite nanoparticles [8] and are encouraging for optimized sensing schemes.

V. References

[1]D A Allwood1, Gang Xiong, M D Cooke, R P Cowburn. Magneto-optical Kerr effect analysis of magnetic nanostructures. Journal of Physics D: Applied Physics. 2003; 36: 2175-2182

[2]"Ferromagnetism." *Wikipedia, The Free Encyclopedia*. 9 Nov 2009, 01:59 UTC. 16 Nov 2009 <http://en.wikipedia.org/w/index.php?title=Ferromagnetism&oldid=324761232>.

[3]Griffiths D. Introduction to Electrodynamics. Upper Saddle River (NJ): Prentice Hall; 1999

[4]"Hysteresis." *Wikipedia, The Free Encyclopedia*. 11 Nov 2009, 19:51 UTC. 16 Nov 2009 <http://en.wikipedia.org/w/index.php?title=Hysteresis&oldid=325298599>.

[5]L. Wang, K. Yang, C. Clavero, A. J. Nelson, K. J. Carroll, E. E. Carpenter, and R. A. Lukaszew. Localized Surface Plasmon Resonance enhanced magneto-optical activity in core-shell Ag-Fe nanoparticles. Submitted, Pending

[6]"Magneto-optic Kerr effect." *Wikipedia, The Free Encyclopedia*. 24 Oct 2009, 19:23 UTC. 16 Nov 2009 <http://en.wikipedia.org/w/index.php?title=Magneto-optic_Kerr_effect&oldid=321805675>.

[7]"Nanoparticle." *Wikipedia, The Free Encyclopedia*. 12 Nov 2009, 12:36 UTC. 16 Nov 2009 <http://en.wikipedia.org/w/index.php?title=Nanoparticle&oldid=325427052>.

[8]Prashant K. Jain, Yanhong Xiao, Ronald Walsworth, and Adam E. Cohen
Nano Lett., **2009**, 9 (4), 1644-1650

[9]Petros Argyres. Theory of the Faraday and Kerr Effects in Ferromagnetics. Physical Review. 1955;97(2): 334-345

[10]"Polarization." *Wikipedia, The Free Encyclopedia*. 13 Nov 2009, 19:51 UTC. 16 Nov 2009 <http://en.wikipedia.org/w/index.php?title=Polarization&oldid=325673642>.

Localized Surface Plasmon Resonance enhanced magneto-optical activity in core-shell Ag-Fe nanoparticles

L. Wang[1], K. Yang[2], C. Clavero[2], A. J. Nelson[1], K. J. Carroll[3], E. E. Carpenter[3], and R. A. Lukaszew[1,2]

[1]*Department of Physics, College of William & Mary, Williamsburg, VA, USA*

[2]*Department of Applied Science, College of William & Mary, Williamsburg, VA, USA*

[3] *Department of Chemistry, Virginia Commonwealth University, Richmond, VA, USA*

Abstract

Metallic nanoparticles (NPs) are suitable platforms for miniaturized bio-sensing based on their optical and magneto-optical properties. It is possible to enhance the sensitivity of specific kinds of NPs by exploiting their optical and magneto-optical properties under suitable external magnetic field modulation. Here, the magneto-optical properties of Fe-Ag core-shell ferromagnet-noble metal NPs have been investigated as function of the incident light frequency. For Fe-Ag NPs with a concentration ratio around 25:75 an optical absorption band centered at 3 eV due to Localized Surface Plasmon Resonance (LSPR) excitation is observed. A strong enhancement of the Faraday rotation is also observed, greatly exceeding the value estimated for pure Fe NPs, also associated with the LSPR excitation. Our findings open up the possibility of highly sensitive miniaturized magneto-optically modulated bio-sensing.

Introduction

Development of highly sensitive biosensors for the diagnosis and monitoring of diseases, drug discovery, proteomics, and environmental detection of biological agents is an extremely significant problem[i]. In addition to the needs for enhanced sensitivity, the development of large-scale biosensor arrays composed of highly miniaturized signal transducer elements that can enable the real-time, parallel monitoring of multiple species imposes stringent requirements for high-throughput screening applications[ii]. Much biosensor research has been devoted to the evaluation of various signal transduction methods including optical, piezoelectric, magnetic, micromechanical, amperometric and mass spectrometric. Although each of these methods has its individual strengths and weaknesses, a strong case has been made that optical sensors, in particular those based on evanescent electromagnetic fields such as propagating Surface Plasmon Polaritons (SPPs) in planar Au and Ag surfaces, are fast becoming a preferred method in many sensing applications[iii]. SPPs are essentially electromagnetic waves that are trapped on the interface of two media with permittivity of different sign, typically between a metal and a dielectric, due to their interaction with the free electrons of the metal[iv]. In addition, SPPs can also appear in appropriately designed metallic and metallo-dielectric structures as Localized Surface Plasmon Resonance (LSPR) that is excited when the incident photon frequency is resonant with the collective oscillation of the conduction electrons. As a consequence, noble metal nanoparticles exhibit a UV-visible absorption band not present in the bulk metal[v,vi], resonant Rayleigh scattering with an efficiency equivalent to that of 10^6 fluorophors[vii], and enhanced local electromagnetic fields near the surface of the nanoparticle[viii]. Plasmon resonances impart these nanostructures with unusual optical properties, such as strongly enhanced size-, shape-, and medium-dependent light absorption and have been employed in a wide range of applications including imaging, chemical and biological sensing and probing with remarkable sensitivity. Thus, several research groups have explored optical biosensors[ix] based on the optical properties of noble metal nanoparticles.

Although quite sensitive for many applications, most current bio-sensing schemes based on Surface Plasmon Resonance (SPR) and LSPR are “passive”, i.e. they are based on changes in the optical properties of the gold-surface when a biological specimen to be detected is bound to it and Surface Plasmons are excited. Thus, to further enhance the sensitivity for more stringent applications, we have explored core-shell “magneto-optically active” plasmonic NPs. Here the magneto-optical property can be varied under application of a modest external magnetic field hence enhancing the NPs inherent sensitivity by using field-modulated detection schemes that exploit their magneto-optical activity. Transition metals such as Fe, Ni and Co alone exhibit magneto-optical effects accessible at relatively low fields, but their absorption coefficients are higher than those of Au or Ag and therefore their SPPs are considerably damped, but when combined with these noble metals their magneto-optical activity is enhanced due to the large electromagnetic fields that arise in the composite nanostructure when sharp SPP is excited in the noble metal[x,xi,xii]. In fact, recent reports have indicated that the combination of noble metal (Au) and magnetic materials (Ferrite) in core-shell magnetic nano-particles exhibit remarkable magneto-optical effects[xiii], suggesting the possibility of implementing magneto-plasmonic materials to enhance sensitivity in bio-detection. In the present case we report on enhancement of the magneto-optical activity observed in core-shell Fe-Ag magnetic NPs due to excitation of LSPR. The spectral absorbance and the magneto-optical Faraday rotation of the polarization of light through a magnetized medium composed of the core-shell Ag-Fe NPs suspended in a suitable liquid between glass slides was observed in transmission geometry.

Experimental

Core shell Ag-Fe magnetic NPs were synthesized by aqueous reduction using sodium borohydride. The synthesis first included reduction of iron nano-particles and was followed by the addition of silver

nitrate. The iron served as a nucleation site for the reduction of silver, creating a core-shell nano-particle. The particles were washed with ethanol several times and magnetically separated using a rare-earth magnet. X-ray powder diffraction revealed a mix phase system with a body centered cubic iron and face centered cubic silver[xiv]. Transmission electron micrographs (TEMs) were taken on a JEOL JEM-1230 at 150 kV with a Gatan Ultra Scan 4000 SP 4Kx4K CCD camera to determine the size, dispersion and morphology of the coated particles. The magnetization reversal was investigated by measuring hysteresis loops at room temperature (RT) on a Lakeshore model 7300 vibrating sample magnetometer. The sample was placed in a gelcap where the background was negligible compared to the sample signal.

For the optical and magneto-optical studies, the magnetic nano-particles were suspended between two glass slides using index-matching oil with n=1.5018. Absorption and Faraday rotation measurements were carried out in the spectral range 1.4 to 3.5 eV. The light incident beam was linearly polarized by a Glan Thompson polarizer (extinction ratio 100,000:1) and then transmitted through the sample. The sample was placed in the gap of an electromagnet with hollow polar pieces, allowing applied magnetic fields up to 1 Tesla, that were high enough to magnetically saturate the NPs. The transmitted light was analyzed by a polarizer positioned at 45º degrees with respect to the incident polarization. The intensity variations were detected using a Si photodetector and lock-in amplifier techniques.

Results and discussion

TEM was performed to determine the size distribution and morphology of the iron-core Fe-Ag NPs. Figure 7 shows a TEM image corresponding to core-shell NPs with a Fe-Ag concentration ratio of 75:25. The inset shows a high resolution TEM image of the Fe-Ag NPs illustrating their core-shell

structure with body centered cubic iron core and face centered cubic silver shell with an average total particle size of 15 nm.

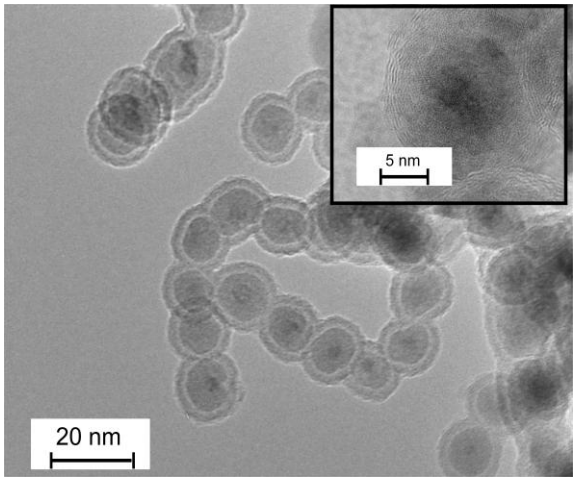

Figure 7. TEM image of Fe-Ag core-shell nanoparticles synthesized by aqueous reduction. The inset shows a high resolution TEM image of the Fe-Ag nanoparticles which illustrates the core-shell structure of the particles with an average particle size of 15 nm.

The magnetic properties were studied by measuring hysteresis loops at RT. As shown in Figure 8, the NPs show characteristic superparamagnetic behavior with very low coercivity and high saturation fields around 5 kOe due to the fact that their volume is well below the critical volume and corresponding superparamagnetic field, which for Fe NPs corresponds to diameters around 26 nm[xv].

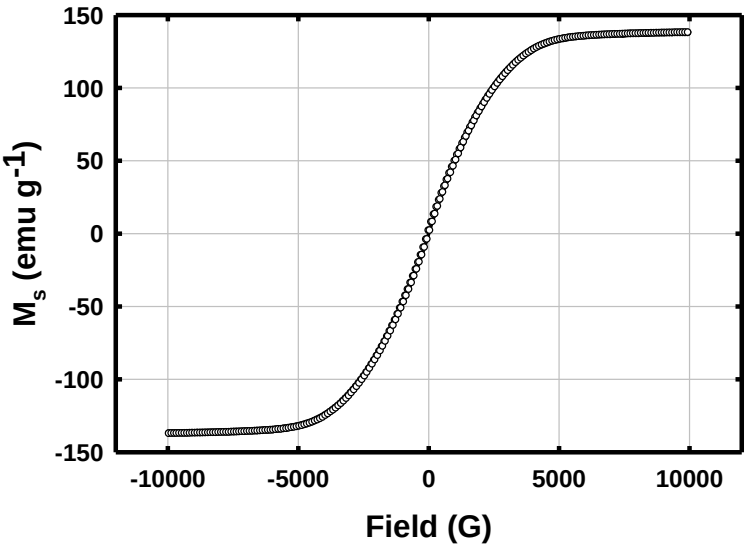

Figure 8. Hysteresis loop for core-shell Ag-Fe nanoparticles showing their superparamagnetic behavior at room temperature, with saturation fields of approximately 5 kOe.

The absorbance and Faraday rotation of the Fe-Ag core-shell nanoparticles suspended in index-matching oil with n=1.5018 were measured in the spectral range from 1.4 to 3.5 eV. As shown in Figure 9 (a) the absorbance of Fe-Ag nanoparticles with a Fe-Ag concentration ration of 25:75 exhibits an absorption band centered at 3 eV, signature of LSPR excitation as shown in previous reports[xiii]. Associated with such absorption band there is a maximum in the Faraday rotation [Figure 9 (a) right]. Simulations of the effective dielectric tensors of the dispersed NPs films were performed using a variation of the Maxwell-Garnett effective medium approximation presented by M. Abe[xvi,xvii] for composite core-shell systems in order to understand the observed behavior. For this study the bulk Fe and Ag optical and magneto-optical constants were used[xviii], since the size of the NPs is well above that at which optical size effects have been described in nanoparticles[xix]. Subsequently, the absorbance and

Faraday rotation were calculated using a matrix transfer formalism[xx,xxi], able to describe the behavior of light in multilayered systems. Figure 9 (b) shows simulations using the cited formalism and considering a 25 % concentration of NPs in the medium (continuous lines). As it can be observed, very good agreement is obtained between the simulation and the experimental data, confirming an absorption band centered at 3 eV and an associated maximum in the Faraday rotation. For comparison, the response of Fe nanoparticles with no coating and simulated under the same conditions is also shown in Figure 9 (b) with dashed lines. Due to the relatively high optical absorption of Fe in the UV and visible range, over-damped or no LSPR excitation is expected. It is worth noting that the experimental measurement of such Fe nanoparticles with no coating cannot be achieved due to the high tendency of Fe to oxide, but their simulated response allows us to understand the effect of LSPR excitation on the optical and magneto-optical properties of core-shell Ag-Fe NPs. In fact, a broader and less intense absorption band is observed as in Figure 9 (b), indicating over-damped or no LSPR excitation. More interestingly, in spite of the fact that in this case the concentration Fe in the nanoparticles is 4 times higher than in the 25:75 Fe-Ag nanoparticles, a much smaller Faraday rotation is observed, thus evidencing a strong enhancement of the magneto-optical response for the Fe-Ag core-shell NPs when the Ag content is higher.

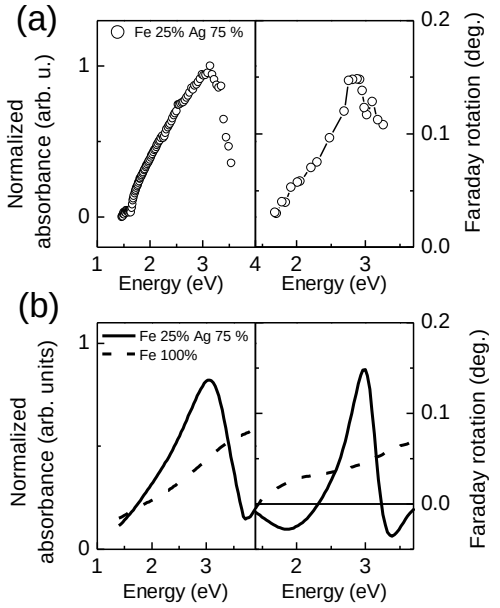

Figure 9. (a) Experimental absorbance (left) and Faraday rotation (right) for 25% Fe-75% Ag nanoparticles suspended in a liquid with n=1.5. A maximum both in absorbance and Faraday rotation is found around 3 eV due to Localized Surface Plasmon Resonance (LSPR) excitation. (b) Simulations show for 25% Fe-75% Ag (continuous lines) and 100 % Fe (dashed lines) nanoparticles show the effect of LSPR on the optical and magneto-optical response of the system.

Conclusions

We have investigated the microstructure, magnetism, optical and magneto-optical properties of Fe-Ag core shell NPs. The nanoparticles exhibit a mix phase system with a body centered cubic iron core and face centered cubic silver shell with average diameters around 15 nm. Superparamagnetic behavior was observed due to their reduced dimensionality. For Fe-Ag nanoparticles with concentration ratio around 25:75 an optical absorption band centered at 3 eV is observed due to LSPR excitation. Associated with such increased absorbance a strong enhancement of the Faraday rotation it is also observed, greatly exceeding the estimated value for pure Fe nanoparticles.

References

[i] A. P. F. Turner, *Science* **290**, 1315-1317 (**2000).**
[ii] A. J. Haes, R. P Van Duyne, *J. Am. Chem. Soc*., **124** (35), 10596–10604 (2002).
[iii] R. Wang, *Biosensors and Bioelectronics* **20***(5)*, 967-974 (2004).
[iv] W. L. Barnes, A. Dereux and T. W. Ebbesen, Nature **424** (6950), 824-830 (2003).
[v] C. L. Haynes, R. P. Van Duyne, *J. Phys. Chem. B **105***, 5599-5611 (2001).

[vi] U. Kreibig, M. Gartz,, A. Hilger, H. Hovel, H. In *Cluster Materials*; Duncan, M. A., Ed.; Advances in Metal and Semiconductor Clusters 4; JAI Press Inc.: Stamford, CT, 1998; pp 345-393.

[vii] M-Y. Ng and W-C. Liu, Optics Express **17**, Issue 7, pp. 5867-5878 (2009), G. C. Schatz, R. P. Van Duyne. In *Handbook of Vibrational Spectroscopy*; Chalmers, J.

M., Griffiths, P. R., Eds.; Wiley: New York, 2002; Vol. 1, pp 759-774.

[viii] R. H. Ritchie, "Plasma losses by fast electrons in thin films" *Phys. Rev.* **106**, 874-881(1957).

[ix] M. D. Malinsky, K. L.Kelly, G. C.Schatz, R. P. Van Duyne, *J. Am.Chem. Soc.* **123**, 1471-1482 (2001), R. Elghanian, J. J. Storhoff, R. C. Mucic, R. L. Letsinger, C. A. Mirkin, *Science,* **277,** 1078-1081 (1997), C. A. Mirkin, R. L. Letsinger, R. C. Mucic, J. J. Storhoff, J. J. *Nature 382*, 607-609 (1996).

[x] J. B. Gonzalez-Diaz, A. Garcia-Martin, G. Armelles, J. M. Garcia-Martin, C. Clavero, A. Cebollada, R. A. Lukaszew, J. R. Skuza, D. P. Kumah and R. Clarke, Phys. Rev. B **76** (15), 153402 (2007).
[xi] G. Armelles, J. B. Gonzalez-Diaz, A. Garcia-Martin, J. M. Garcia-Martin, A. Cebollada, M. U. Gonzalez, S. Acimovic, J. Cesario, R. Quidant and G. Badenes, Optics Express **16** (20), 16104-16112 (2008).
[xii] C. Hermann, V. A. Kosobukin, G. Lampel, J. Peretti, V. I. Safarov and P. Bertrand, Phys. Rev. B **64** (23), 235422 (2001).
[xiii] P. K. Jain, Y. H. Xiao, R. Walsworth and A. E. Cohen, Nano Letters **9** (4), 1644-1650 (2009).

[xiv] S. Naik, E. E. Carpenter, J. Appl. Phys. **103**, 07A313 (2008).
[xv] C. M. Boubeta, C. Clavero, J. M. Garcia-Martin, G. Armelles, A. Cebollada, L. Balcells, J. L. Menendez, F. Peiro, A. Cornet and M. F. Toney, Physical Review B **71** (1), 014407-1 (2005).
[xvi] M. Abe and J. Kuroda, J. .Appl. Phys. **91** (10), 7305-7307 (2002).
[xvii]M. Abe and T. Suwa, Phys. Rev. B **70**, 235103 (2004).

[xviii] E. D. Palik, *Handbook of optical constants of solids*. (Academic Press, Orlando, 1985).
[xix] C. Clavero, A. Cebollada, G. Armelles, Y. Huttel, J. Arbiol, F. Peiro and A. Cornet, Phys. Rev. B **72** (2), 024441 (2005).
[xx] M. Schubert, Phys. Rev. B **53** (8), 4265 (1996).

[xxi] M. Schubert, T. E. Tiwald and J. A. Woollam, Appl. Opt. **38** (1), 177-187 (1999).